Journal of Applied Fluid Mechanics, Vol. 13, No. 3, pp. 1047-1054, 2020.
Available online at www.jafmonline.net, ISSN 1735-3572, EISSN 1735-3645.
DOI: 10.29252/jafm.13.03.30466

Numerical Study of Water Vapor Injection in the Combustion Chamber to Reduce Gas Turbine Fuel Consumption

R. Sharafoddini[1], M. Habibi[2] and M. Pirmohammadi[3†]

[1] *Department of Mechanical Engineering, Tehran Gharb branch, Islamic Azad University, Tehran, Iran*
[2]*Energy Technologies Research Division, Research Institute of Petroleum Industry (RIPI), Tehran, Iran*
[3]*Department of Mechanical Engineering, Pardis Branch, Islamic Azad University, Pardis, Iran*

†*Corresponding Author Email: pirmohamadi@pardisiau.ac.ir*

(Received May 1, 2019; accepted November 2, 2019)

ABSTRACT

In this study, the effect of water vapor injection on the flow pattern, temperature contamination and emission of pollutants has been studied. Also, the impact of the spray angle on the axis has been investigated and finally, the effect of fuel type and geometry on the flow variables has been investigated. The results were compared with numerical simulations performed by other researchers and the results showed that they are qualitatively acceptable. The purpose of this work is to investigate the effect of the amount of water vapor on flame and NO_x released from combustion. The results showed that with the percentage of water injected, there were significant changes in the temperature and pressure contour patterns of the combustion chamber. The results showed that with the percentage of water injected, there were significant changes in the temperature and pressure contour patterns of the combustion chamber. The results showed that the overall efficiency of the Brighton cycle can be increased in the non-injecting mode from 91% to 95% for the combustion chamber mode by injecting 8% water vapor. Also, an increase of more than 8% of water vapor will not have much effect on efficiency of gas turbine and reduce fuel consumption.

Keywords: Combustion chamber; Water vapor injection; Pollution release; Hexane; Fluent; Computational fluid dynamics.

1. INTRODUCTION

The gas turbine is a rotary machine based on the energy of combustion gases. Each gas turbine includes a compressor for compressing air molecules with the help of a number of fixed and moving blades, A combustion chamber for mixing fuel with compressed air, And turning it off and a turbine to convert the mechanical energy generated in the turbine, Spinning the compressor itself is turbine and the remaining energy, depending on the use of gas turbine, The turbo generator rotates the electric generator (turbo jet and turbofan) Or directly (or after changing the gearing speed) using the same way (turbocharged, turbo-prop, and turbofan). Today, modern gas turbines are widely used to generate electricity or as propulsion engines on planes. And, considering the amount of gas consumed by gas turbines, these tools are one of the main sources of CO and NOx combinations of hydrocarbons. Therefore, due to the harmful effects these compounds have on human health and the environment and also due to strict environmental there are regulations for the use of these devices. The requirement to optimize and reduce the fuel consumption of these devices has a huge impact on improving these conditions. In addition, in terms of the difficulty and the cost of experimental methods proposed using of numerical methods to predict the behavior of the combustion chamber of gas turbines (El, 1984)

Nishida *et al*. (2005) analyzed the performance of two types of regenerated steam injection turbine (RSTIG) and compared their performance with simple, reduced, turbine, water vapor and water vapor injection (STIG). Their results showed that the thermal efficiency of RSTIG systems was higher than the regenerated systems, water injection and STIG and their special power is higher than the revived cycle. The optimal pressure ratio for the maximum RSTIG system efficiency is relatively low. Therefore, the status of water vapor injection can be applied in the systems of simultaneous generation of heat and flexible power and the overall

efficiency of the RSTIG synchronous system will exceed more than 70%. Xue *et al* (2016) investigated the effect of water vapor on the combustion process inside the combustion chamber. They completed the operation of the gas turbine with the design of the combustion chamber and formulated a detailed procedure for single-ring combustion chambers with careful attention by steam added.Model predictions were compared with data from the real engine and their results had good accuracy. Zhang *et al*. (2015) calculated the performance of the partial oxidation gas turbine (POGT) with steam turbine cycle (STIG) and examined the overall performance of these cycles and the effects of their key variables. Their calculation results showed that the outlet temperature of the combustion chamber and the compressor pressure ratio of the lower gas turbine cycle, and the partial oxidation temperatures, clearly affect the efficiency and output of this cycle. Tumacock *et al*. (2002) conducted a study on the flame penetration of the combustion chamber of a gas turbine fed by combining natural gas and hydrogen. CFD studies were conducted with the help of FLUENT. from pure gas to pure hydrogen. They concluded that by modifying the composition of fuel, the NOx emission level showed a significant increase, while the temperature distribution of the material changed slightly. The calculated static gas temperature of natural gas and its composition to pure hydrogen are shown in the Fig. 1.

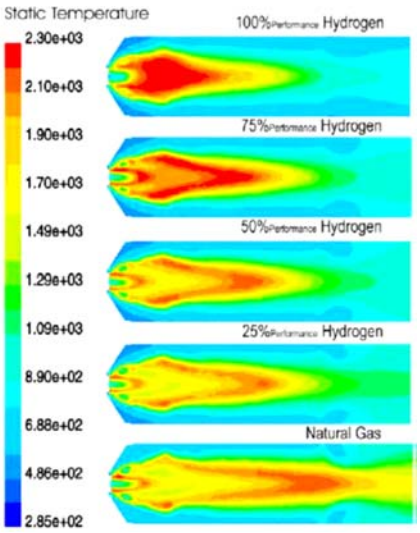

Figure 1: Contours of static temperature for natural gas, mixture and pure hydrogen

All of these calculations were obtained for a fixed performance of about 8.6 MW (baseline load conditions).By increasing the hydrogen contribution, a significant change in the shape of the flame can be seen. The results showed that the hydrogen flame was more compact and shorter and its temperature was higher. While the widest hot zone was from burning natural gas right in front of the dilapidated area, and the region of the highest burning temperature of hydrogen was downstream of the stream towards the front of the combustion chamber (in the inlet direction of the gas). The highest temperatures with pure hydrogen burning are about 2330 degrees Kelvin, while using natural gas at about 2290 degrees Kelvin.

In 2013, Shabanian *et al* (2013) used Flamelet and PDF models for combustion with a turbulence k-ε model and two kinetic mechanisms GRI-Mech 3.0 and POLIMI to numerically measure jet-ethylene flame combustion. Mardani *et al* (2016) examined the combustion chamber of a gas turbine in 2016 using two different reaction models, EDC and TPDF. In this simulation, DRM22 have been investigated with 22 chemical species and 227 reactions. The EDC method works better than the TPDF at the bottom of the combustion chamber, and it is more accurate to predict the maximum temperature and the main species (CO2, O2, H2, and H2O). In 1986, Burnham *et al*. (1986) reported that the addition of excess air is an effective way to reduce NOX, but is not widely used because of the increase in the flow rate in the initial region and the effect on flame stability. The first idea of steam injection into gas turbine cycle was introduced in 1903. Numerical simulation of the combustion chamber has done by Jones *et al* (1979), which illustrate common simplifications and important issues in the simulation of the combustion chamber. In 1978, Jones and Predin provided a three-dimensional solution for the flow and temperature and concentration of mass samples for a liquid fuel combustion chamber. Ayadian and Mazaheri (2016) examined steam injection into the chamber and pre-mixed with fuel, and its results were compared with the non-injector mode into the chamber and the vapor injection mode pre-mixed with air. The injection of steam into the combustion chamber is accomplished by increasing the mass flow through the nozzle diameter increase at a constant input speed. The results show that injection of precooked vapor with fuel contributes 8.5% and 7.4%, respectively, to NOx and CO emissions relative to the premixed vapor injection. The main purpose of steam injection into a gas turbine cycle was initially to increase the output power by increasing the mass flow rate of the cycle. However, according to studies conducted by Shaw *et al*. (1974) it was found that steam injection reduces the temperature of the combustion chamber, reducing the nitrogen oxides produced in the gas turbine. Aissani *et al*. (2007) examined the effect of steam injection on the performance and pollutants of the gas turbine cycle, In this study, the thermodynamic analytical relationships for the gas turbine cycle and the semi-experimental relations for pollutants, the thermodynamic characteristics of the cycle and the amount of pollutants were calculated and analyzed by the injection of steam into the compartment of the effect of this parameter. The results show that steam injection improves cycle performance, decreases NOx production of the enclosure and increases carbon monoxide. Almeida *et al*. (2019) developed a model for the prediction of air entrainment in a full-premix, atmospheric, ejector-pump like gas burner, used for domestic water heating purposes.

The model improves current knowledge by including

the Effects of combustion and buoyancy on the air entrainment mechanism. It predicts burner geometry, type of hydrocarbon fuel and burner firing rate. Asgari *et al*. (2017) investigated the effects of a fuel injection strategy on performance the premixing chamber of the Modern Dry-Low-Emission (DLE) Gas-Turbine (GT) combustors. An Eulerian-Lagrangian model for multi-phase multi-component flows is evaluated and used to investigate the effects of different fuel spray design parameter, including injection location, direction, mass-flow-rate partitioning, and flow-swirl number, is the performance of the premixing chamber.

Farokhipour *et al*. (2018) used an Eulerian-Lagrangian model is implemented to study the process of water spray injection inside gas turbine combustors. Amani *et al*. (2018) studied the water spray injection process in a natural-gas-fueled gas turbine combustor numerically using an Eulerian-Lagrangian formulation, and the combined effect of different design variables, including the swirl number, water injection mass flow rate, injection partitioning between a pre- and a post-flame injector, and injection direction, are investigated on several

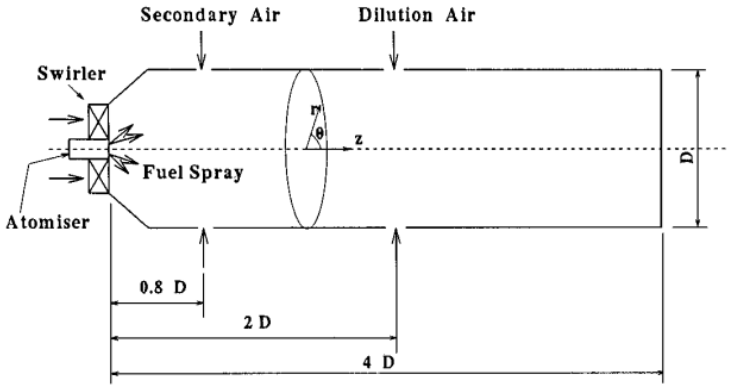

Fig. 2. Schematic diagram of combustion chamber model.

Fig. 3. Combustion chamber mesh.

combustor performance objectives by systematic multi-objective optimizations.

2. MODELING AND MESH OF THE COMBUSTION CHAMBER

The schematic of the combustion chamber is shown in the Figure 2. The combustion chamber consists of three parts: The first air inlet nozzles and fuel, the second part is the body of the chamber and the third part of the exhaust is located at the end of the combustion chamber. The injector consists of a nozzle for central air and a nozzle for fuel and a nozzle for external airflow. Both air nozzles provide a rotating air under the environment of a plenum. The diameter of the central air nozzle is 0.1D and the inner diameter of the nozzle is 0.1 D and its outer diameter is 0.2 D. It is assumed that the inlet air through the central nozzle is supplied about 40% of the total air. It is also assumed that the fuel is injected under non-rotating conditions. The diameter of the main body of the combustion chamber is D and its height is 4D.

Also, in the exhaust of the combustion chamber is located an exhaust at the same diameter D.

To reduce the dimensions of the problem from three dimensions to two dimensions, one can use the pivot symmetric condition. Also, since the air in the above problem is inverted, a two-dimensional rotary pivot symmetric condition is used to simulate the field. The first step is to simulate numerical flow of network fluid flow. The problem of networking has a great influence on the answers. There are many software in the field of networking, among which GAMBIT software has some special features.

In the fluid field network, this software has been used for this software. Since the geometry is a regular geometry, a systematically organized grid is used to network the problem. In this way, the most suitable elements are constructed according to the geometry of the problem. Elements used in the production of a rectangular grid are presented in the Fig.3

As shown in this figure, the grid near the fuel nozzle is thinner so that the accuracy of the calculations increases and the computational error reaches its lowest value.

3. EQUATIONS

In this section, the equations of fluid flow and combustion are presented. These equations include the mass survival equation, Navier-Stokes equations, energy conservation equations, and equations for turbulence models. The momentum equation is considered only in the continuous state; therefore, we have for an incompressible flow (1986):

Conservation of mass equation:

$$\frac{\partial U_i}{\partial x_j} = 0 \tag{1}$$

Navier-Stokes equation:

$$\frac{\partial (U_j U_i)}{\partial x_j} = \frac{1}{\rho}\frac{\partial p}{\partial x_i} + \frac{\partial}{\partial x_j}\left(\nu \frac{\partial U_i}{\partial x_j} - \overline{u'_i u'_j}\right) \tag{2}$$

Here, the statement $u'_i u'_j$ is unknown and is known as the Reynolds tension. The well-known model of the Reynolds approximation is based on the Businisk hypothesis, which assumes that the Reynolds tensor is proportional to the strain rate tensor and is expressed as follows.

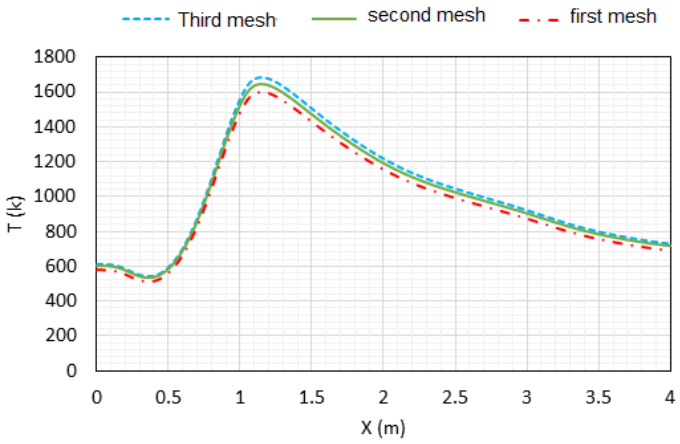

Fig. 4. Independent resolution of the network.

$$\overline{u'_i u'_j} = \nu_t\left(\frac{\partial U_i}{\partial x_j} + \frac{\partial U_j}{\partial x_i}\right) - \frac{2}{3}k\delta_{ij} \tag{3}$$

In Eq. (3) ν_t, the viscosity of vortex and k is the kinematic energy of turbulence defined as follows, and δ_{ij} is the Kronecker delta:

$$k = \frac{\overline{u'_i u'_j}}{2} \tag{4}$$

The viscosity of the vortex, ν_t, in the system SI is m^2 / s. The conventional methods for defining ν_t are the combination of kinetic energy of turbulence, k, and dispersion distribution rate ε, $\nu_t = ({}^{C_\mu k^2}/_{\varepsilon}\ 2)\ /\varepsilon$, or the combination of kinetic energy of turbulence with the specific dispersion distribution rate ω, $\nu_t = {}^{k}/_{\omega}$. Therefore, additional dual transfer equations for k and ε, or k and ω are needed to complete the set of equations described above. In this study, the turbulence model K-ε standard is used for turbulence modeling.

Energy survival equation:

The energy conservation equation is given as a priori:

$$\frac{\partial}{\partial x}(\rho E) + \nabla.\left(\vec{v}(\rho E + p)\right) = \nabla.\left(k_{eff}\nabla T - \sum_j h_j \vec{J}_j + \left(\bar{\bar{\tau}}_{eff}.\vec{v}\right)\right) + S_h \tag{5}$$

In the above equation, k_{eff} is a thermal conductivity coefficient. (k + k_t, where k_t is the thermal conductivity of the turbulence and enters the equations when the turbulence model is used).

$\vec{J}_j$ is defined as the j diffusion. The three first-order of the equation above represent the heat transfer, as a result of conduction, species penetration and viscous loss. S_h contains heat from chemical reactions and other volumetric thermal sources.

4. NUMERICAL METHOD

The inflow of air is assumed to be uncontrolled with a uniformly rotating speed in the flow field. The operating fluid is intended to simulate numerical flow, air composition and hexane fuels. The flow with constant temperature and velocity enters the computational domain. The equations in the steady state are given in relations (1) to (5). It should be noted that the numerical solution of thermal conductivity is considered pivotal.

For the discretization of the equations, the accuracy of the second-order Euler method is used. Also, to break the penetration sentence, for the same reason, the second-order central limit difference method has been used. In the reports presented in this study, the SIMPLE algorithm is used to connect the speed and pressure field. In order to model the turbulence component in the equations, a standard k-ε model is used here. Also for controlling the equations, the

control volume technique is used in the implicit state. Here, the hydraulic and thermal flow of the flame is assumed to be in constant state. It should be noted that here the energy equation is also disjoint to achieve higher accuracy using a finite difference of second order. Since the volume of calculations has a direct relation to the size of the grid, first we must consider the most suitable network size for the computational field. Three different types of networks have been selected for this purpose.

4.1 Grid Independency

For this purpose, first the grid independency must be investigated. As a result, the temperature variations of the combustion chamber are plotted in terms of longitudinal position (Fig. 4). As it stands, the difference between the results of the second and third grid is very close. As a result, the type II grid was used in this project.

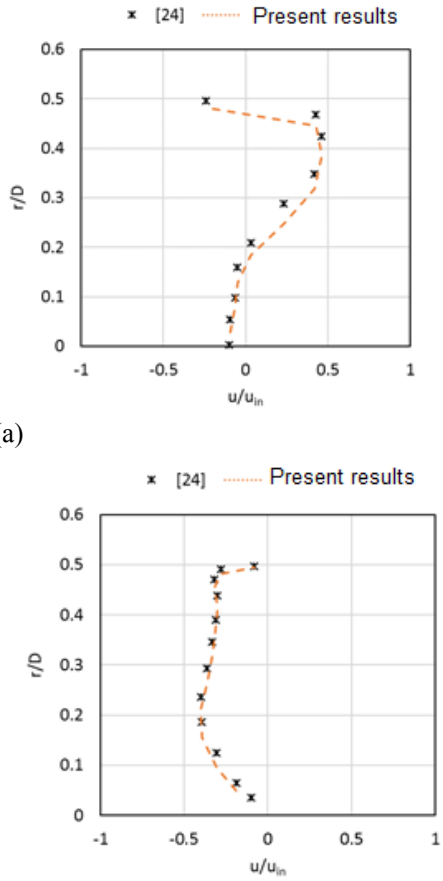

(a)

(b)

Fig. 5. Comparison of speed components calculated by the present work and numerical simulation. A) axial component, B) radial (swirl) cross section x = 0.75 m.

4.2 Verification of Simulation

In order to verify the resolution for the two models considered in this study, the symmetric geometry of the pivot combustion chamber with similar dimensions and geometry is simulated and modeled in which the pivot, radial and rotational velocities in a uniform cross section of the compartment combustion has been compared with numerical results from the present study. In the following figure, we can see the comparison between the components of the axial and swirling speeds at a cross section of x = 0.75m in comparison with the model.

As it is clear the difference between the results is negligible. To calculate the difference in the results, we will examine the absolute magnitude of the difference between the points in the numerical results with the present study. It can be seen that the difference between the results for axial and radial velocities respectively is about 1.35% and 0.65%.

Also to ensure more reliable results, the dimensionless temperature contour from the current study will be compared with the results reported by (1991).

As it is shown in Fig.6, qualitatively the results are consistent. The reason for the slight difference is due to difference in the numerical method and the assumptions.

5. DISCUSSION AND RESULTS

5.1 Influence of water vapor injection on combustion

Modeling of disturbance and kinetic confinement is one of the most complex parts of the combustion chamber modeling. Selection of a suitable combustion model with respect to the time of solving and predicting the production of the compartment is very important. In the present study, it is assumed that the amount of water vapor into the combustion chamber is added to the fuel injected. The purpose of this work is to investigate the effect of water vapor concentration on flame and combustion material. The temperature contour in the combustion chamber is shown in Fig.7.

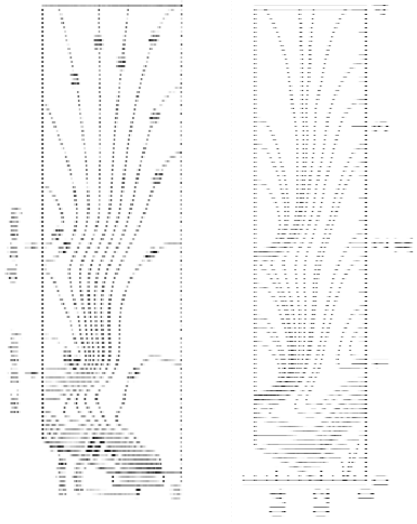

b a

Fig. 6: Comparison of the dimensionless temperature contour calculated by the present work and numerical simulation

As can be seen, with the percentage of water injected, there are significant changes in the temperature profile of the combustion chamber. With an increase in the percentage of water vapor up to 4%, the flame core is lowered and shift towards the beginning of the compartment and this behavior continue to 8% water injection . It is observed that with increasing water vapor up to 12%, the temperature pattern of the flame does not change very much.

The results showed that in Fig.8, the overall efficiency of the Brighton cycle can be increased from 91% to 95% by injecting 8% water.

In the Fig.8, the Nox concentration can be seen from the combustion chamber in ppm, which is normalized by eliminating water molecules. According to Fig.8 it is clear that with increasing mass ratio of water vapor to inlet air from 0.05 to 0.1 the Nox outlet was increased from the combustion chamber due to the breakdown of the water molecules and the increase of the combustion chamber temperature.

However, with an increase in water vapor inlet, outlet NOx from chamber reduces, so that in a mass ratio of 0.2, a significant difference between the output NOx in the non-injecting water vapor ($\dot{m}_w / \dot{m}_a = 0$) and the injection mode of water vapor ($\dot{m}_w / \dot{m}_a = 0.2$) is observed.

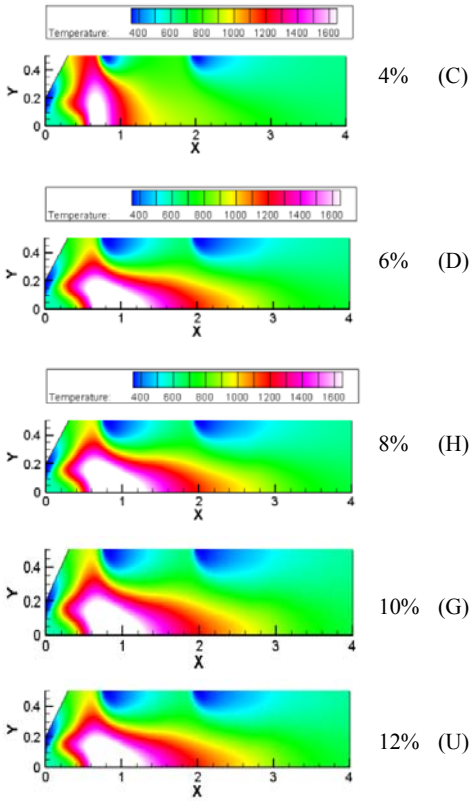

Fig. 7. Effect of water vapor injection on the distribution of temperature contour in the combustion chamber.

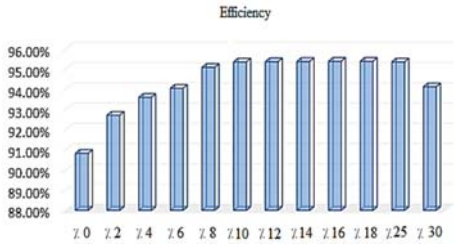

Fig. 8: Effect of steam injection on the efficiency of the Bryton cycle.

5.2 Impact of Air flow Angle on Combustion Pattern

In this section, the effect of the intake airflow angle on the combustion pattern will be investigated. This test will be done for four different angles of 45, 50, 55 and 60 degrees relative to the combustion chamber axis. Other parameters and boundary conditions are the same for all experiments and are similar to those considered in the previous one. As it is known, changes in the core pattern of the rotational wind angle increase. These changes can be seen in Fig. 10.

5.3 Effect of Fuel Type on Combustion Pattern

This section examines the effect of fuel type on ignition pattern. For this purpose, we will introduce three different types of fuels with the names of chemical hexane (C6H14), butane (C4H10) and octane (C8H18). Figure 11 shows the thermal pattern (temperature contour) for these three types of fuel under the same conditions.

As can be seen from Fig. 11, in the case of butane fuel, the flame is drawn toward the body of the combustion chamber, as the octane fuel is observed, the length of the flame is shorter but the core becomes hotter. This is because of the number of carbon atoms in the fuel molecule. Bhutan has lower carbon content than hexane and octane. A large number of carbon atoms in the fuel molecular chain will increase the flame core in the combustion chamber.

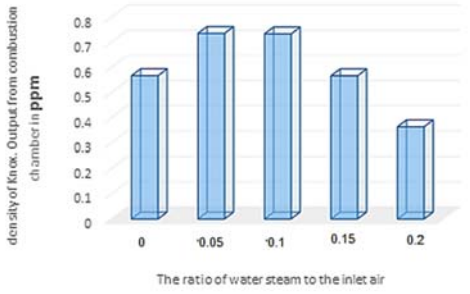

Fig. 9. NOx concentration. Output from combustion chamber in ppm.

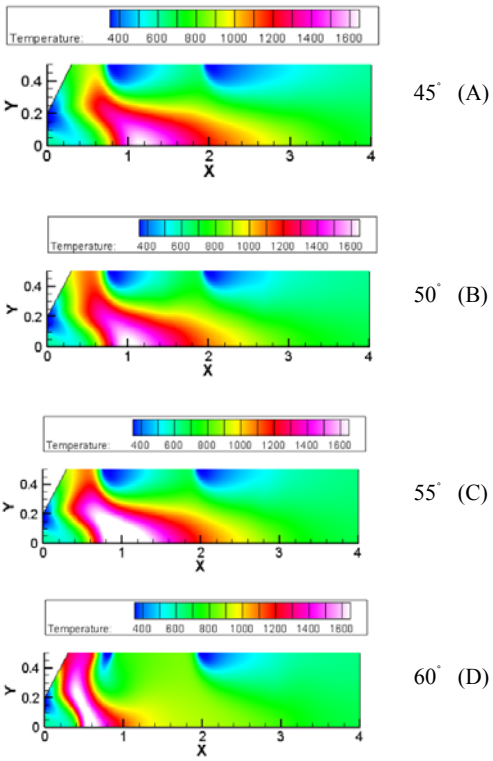

Fig. 10. Effect of the intake air rotating angle on the temperature distribution in the combustion chamber.

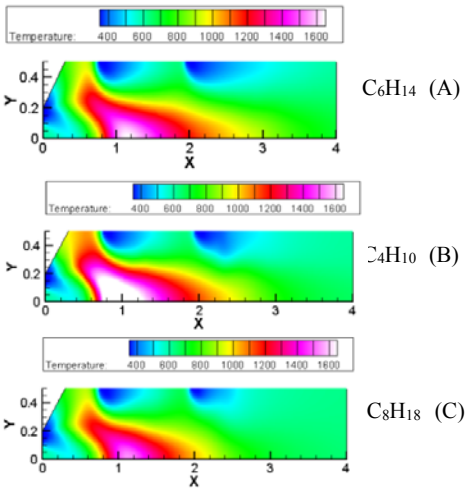

Fig. 11. Effect of fuel injection type on the distribution of temperature in the combustion chamber.

In Fig. 12, the Nox distribution (in ppm) is plotted in the axis of symmetry of the combustion chamber. As it is known, the amount of Nox from the beginning of the combustion chamber to the position near the flame core is approximately equal to zero then this amount increases in the flame core of the combustion chamber and after passing through this region, the amount of Nox decreases to the outlet of the combustion chamber. It can be seen that the change in fuel type only affects Nox at the core of the flame and does not affect other areas.

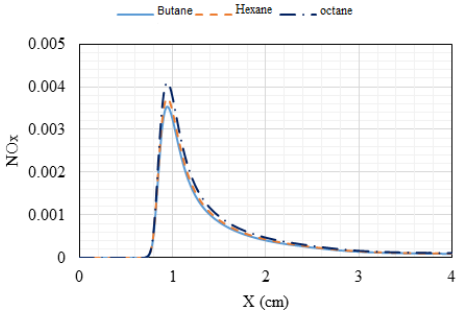

Fig. 12. Effect of fuel type on the distribution of Nox in the combustion chamber axis.

5. CONCLUSION

The purpose of this work is to investigate the effect of the amount of water vapor on flame and Nox released from combustion.

The following conclusions were drawn:

- The results showed that with the percentage of water injected has significant effects on the temperature profile of the combustion chamber.
- By increasing the percentage of water vapor up to 4%, it is observed that the flame core decreases and moves towards the top of the chamber.
- The NOx changes in exhaust emissions were compared with the percentage of water vapor injection. The results showed that the NOx concentration of the output increases in the direction of the combustion chamber axis.
- The region of temperature near the nozzle of water vapor injected changes the temperature field and with the injection of water vapor, the temperature in this area decreases.
- The number of carbon molecular chains caused a significant change in the combustion pattern. In the case of butane fuel, it is seen that the flame is drawn toward the body of the combustion chamber, while in the case of the octane fuel, the length of the flame is shorter but the core becomes hotter. This is because butane has lower carbon content than hexane, and octane has more carbon content than hexane, and more carbon in the fuel molecule chain increases the flame core in the combustion chamber.

REFERENCES

Almeida, A. L. M. de Soto, R. M. Laranjeira, Luís M. Pacheco Monteiro, A. dos Santos and E. Caetano Fernandes, 1D model for a low NOx ejector-pump like burner. *Experimental Thermal and Fluid Science* 100 (2019) 171–192

Amani, E., M. R. Akbari and S. Shahpouri (2018). Multi-objective CFD optimizations of water spray injection in gas-turbine Combustors. *Fuel* 227, 267–278.

Asgari, B. and E. Amani (2017). A multi-objective CFD optimization of liquid fuel spray injection in dry-low-emission gas-turbine combustors. *Applied Energy* 203 696–710

Burnham, J. B., M. H. Giuliani and D. J. Moeller (1986). Development, Installation and Operating Results of a Steam Injection System (STIG™) in a General Electric LM5000 Gas Generator. *in ASME 1986 International Gas Turbine Conference and Exhibit*. American Society of Mechanical Engineers.

El, W. M. (1984). *Power Plant Technology*. McGraw-Hill International.

Farokhipour, A., E. Hamidpour and E. Amani (2018). A numerical study of NOx reduction by water spray injection in gas turbine combustion chambers. *Fuel* 212, 173–186.

Jones, W. and C. Priddin (1979). Predictions of the flow field and local gas composition in gas turbine combustors. *in Symposium (International) on Combustion*. 1979. Elsevier.

Kadi, R., A. Bouam and S. Aissani (2007). Analyze of gas turbine performances with the presence of the steam water in the combustion chamber, *Revue des Energies Renouvelables ICRESD-07 Tlemcen*, 327 – 335.

Mardani, A. and A. Fazlollahi-Ghomshi (2016). Numerical Investigation of a Double-Swirled Gas Turbine Model Combustor Using a RANS Approach with Different Turbulence–Chemistry Interaction Models. *Energy & Fuels* 30(8), 6764-6776.

Mauß, F., D. Keller and N. Peters (1991). A lagrangian simulation of flamelet extinction and re-ignition in turbulent jet diffusion flames. *in Symposium (International) on Combustion*. 1991. Elsevier

Nishida, K., T. Takagi and S. Kinoshita (2005). Regenerative steam-injection gas-turbine systems. *Applied Energy* 81(3), 231-246.

Sayadian, S. and K. Mazaheri (2016). Reducing NOx production of gas turbine combustion chamber with steam injection using the CLN method. *Amir Kabir Mechanical Engineering Magazine* 48 (3), 247-256.

Shabanian, S. R, P. R. Medwell, M. Rahimi, A. Frassoldati and A. Cuoc (2013) Kinetic and fluid dynamic modeling of ethylene jet flames in diluted and heated oxidant stream combustion conditions. *Applied Thermal Engineering* 52(2),538-554.

Shaw, H. (1974). The effects of water, pressure, and equivalence ratio on nitric oxide production in gas turbines. *Journal of Engineering for Power* 96(3), 240-246.

Tomczak, H. J., G. Benelli, L. Carrai and D. Cecchin (2002). Investigation of a gas turbine combustion system fired with mixtures of natural gas and hydrogen. *IFRF Combustion Journal, Article Number: 20020*.

Xue, R., H. Chunbo, V. Sethi and T. Nikolaidis (2016) Effect of steam addition on gas turbine combustor design and performance. *Applied Thermal Engineering* 104, 249-257.

Zhang, S. J., J. L. Chi and Y. H. Xiao (2015). Performance analysis of a partial oxidation steam injected gas turbine cycle. *Applied Thermal Engineering*, 622-629.